J Electr Eng Technol.2018; 13(4): 1549-1557
http://doi.org/10.5370/JEET.2018.13.4.1549

ISSN(Print) 1975-0102
ISSN(Online) 2093-7423

A Novel Region Decision Method with Mesh Adaptive Direct Search Applied to Optimal FEA-Based Design of Interior PM Generator

Dongsu Lee*, Byung Kwan Son, Jong-Wook Kim*** and Sang-Yong Jung†**

Abstract – Optimizing the design of large-scale electric machines based on nonlinear finite element analysis (FEA) requires longer computation time than other applications of FEA, mainly due to the huge size of the machines. This paper addresses a new region decision method (RDM) with mesh adaptive direct search (MADS) for the optimal design of wind generators in order to reduce the computation time. The validity of the proposed algorithm is evaluated using Rastrigin and Goldstein-Price benchmark function. Moreover, the algorithm is employed for the optimal design of a 5.6MW interior permanent magnet synchronous generator to minimize the torque ripple. Additionally, mechanical stress analysis as well as electromagnetic field analysis have been implemented to prevent breakdown caused by large centrifugal forces of the modified design.

Keywords: Interior PM generator, Mechanical stress, Mesh adaptive direct search, Optimal design, Region decision method

1. Introduction

Recently, large-scale electric machines such as wind generators, solar power generators and power transformers have been required to develop alternative energy sources owing to increased power demands. Among them, wind generators, in particular, have been studied and developed thanks to their advantages in terms of the possible installation sites and greater annual energy production compared to other renewable energy sources.

From the perspective of designing wind generators, various operating characteristics need to be considered and therefore thorough numerical techniques of analysis and design are required [1, 2]. Moreover, using finite element analysis (FEA) for rigorous electromagnetic simulations leads to long computation time. Hence, it is necessary to develop a specialized optimal design method suited for large-scale wind generator design.

Mesh adaptive direct search (MADS) is a stochastic local optimum search algorithm that spreads neighbor solutions around the current optimal point to find the more improved one and iterate it [3]. In our previous works, we developed improved versions of MADS called the guided MADS and the variable MADS, in order to obtain the global optimum with faster convergence when optimally designing various electrical machines [4, 5].

A multistart strategy can be applied to MADS for the purpose of expanding it to global optimization. Each of the initial points finds a local optimum in serial order. Then, the most optimal solution is selected. In the case where the convergence path of each multistart is similar, the converged local optima are likely to be identical to each other. For this reason, the convergence time becomes slow due to the unnecessary computations.

This paper presents a new combination of region decision method (RDM) with MADS for the optimal design of a wind generator, where RDM is newly implemented in order to solve these problems. The proposed algorithm improves the convergence speed by saving the search paths and omitting overlapping areas. We analyze the whole search region by using these paths. Additionally, if the difference between the cost value and current optimal solution is large at the same mesh size for each searching path, which means that there is a low probability of including the global optimum, then the current search will stop. This algorithm is highly effective and reliable when it is applied to the problems whose cost function is multimodal, such as the electric machine design problem. In particular, the proposed RDM with MADS has been verified through benchmark functions such as the Rastrigin function and the Goldstein-Price function, both of which contain many local optima and traditionally require much longer computation time.

For optimal design, the employed type of wind generator is the interior permanent magnet synchronous generator (IPMSG). With the benefit of the PM configuration of IPMSG, buried in the rotor, it has advantages in terms of high power density and efficiency compared with other types of generator. However, IPMSGs have the distinctive feature of nonlinear magnetic saturation near PMs [6]. With magnetic saturation, the changing flux according to

† Corresponding Author: School of Electronic and Electrical Engineering, Sungkyunkwan University, Korea. (syjung@skku.edu)
* School of Electrical and Computer Engineering, University of Illinois at Urbana-Champaign, USA. (yama20000@naver.com)
** School of Electronic and Electrical Engineering, Sungkyunkwan University, Korea. (byeongkwani@naver.com)
*** Dept. of Electronic Engineering, Dong-A University, Korea. (kjwook@dau.ac.kr)
Received: July 25, 2017; Accepted: January 29, 2018

rotor position gives rise to the torque ripple [7]. The increasing torque ripple cause various problems in terms of total harmonic distortion of electromotive force, noise and vibration [8]. Hence, it is necessary to reduce the torque ripple by optimal design. In particular, in the case of a large-scale generator, mechanical running circumstances will change greatly according to the modified designs because of the large centrifugal forces [9]. Therefore, it is recommended to include the mechanical stress analysis in order to prevent a breakdown when designing the large-scale generator. In this paper, the optimal design of a 5.6MW IPMSG is executed to minimize the torque ripple combined with a mechanical stress analysis employing the proposed algorithm, which is synthetically based on FEA.

2. Region Decision Method with MADS

2.1 Multistart with MADS

MADS is an iterative optimization method that has reliable and fast convergence to local minima. MADS generates a mesh frame based on the current point and then produces stochastic neighborhood points near the current point in the mesh frame. If at least one of the neighborhood points is an improved one, it is defined as a new frame center. Then, it regenerates a new mesh frame and iterates the search again. If there is no better solution among the neighborhood points, the mesh size is decreased and the neighborhood points are evaluated by the objective function on a more dense mesh with reference to the frame center. Various search strategies are allowed on account of the neighborhood points which are generated randomly on the basis of the mesh frame.

Fig. 1 shows the local search scheme of MADS. Considering that the current solution (x_k) is a frame center, the mesh frame near the frame center is generated by means of the mesh size parameter (Δ_k^m). The poll size parameter (Δ_k^p) dictates the magnitude of the distance from the trial points to the current solution. In accordance with the characteristics of MADS, the trial points on the mesh are defined as [10]:

$$P_k = \left\{ x_k + \Delta_k^m d : d \in D_k \right\}, \tag{1}$$

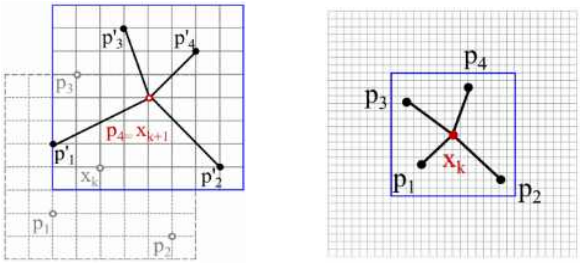

(a) Iteration of the search (b) Mesh frame and poll size parameter

Fig. 1. Conception of MADS frame

where p_k is a set of solutions used to evaluate the objective function and D_k is a positive spanning set for the mesh. The mesh size parameter has the following relationship at the k+1th iteration:

$$\Delta_{k+1}^m = \tau^{\omega_k} \Delta_k^m, \tag{2}$$

where τ is 1/4. ω_k is 0 or -1 for an improved solution and otherwise 1.

Since MADS has the disadvantage of quickly converging to a local minimum, multistart combined with MADS is adopted to enable the exploration to proceed to global optimization. Multistart is classified as an iterative local search method to locate a global minimum which is the best one among the local minima found so far.

In MADS, there are two conditions; the stopping and termination conditions. The stopping condition is necessary to decide whether the current MADS should be continued. In the case where the maximum number of iterations is exceeded or the mesh size drops below the tolerance value, MADS stops the local search and multistart obliges MADS to start from another initial point. The termination condition concerns whether the global minimum is located. The global minimum is already known in benchmark function optimization and is assigned a desired cost value in general problems.

2.2 Search region encoding

Most engineering problems, including the optimal design of electric machines, have multiple solutions whose cost values vary to some extent. For the efficient global optimization of the multimodal cost function, revisiting the solution regions previously sought needs to be prohibited in the exploitation phase. In the exploration phase, however, a large step size makes the search path of the incumbent point pass through those regions, which has to be allowed for search diversification.

The revisiting check has difficulty from two perspectives; registering the regions of local minima found so far and referring to them to protect revisits of the current search path. It is in general difficult to register areas near the local minima in a real-valued search space whose axis scales are different and to decide whether the incumbent point has intruded into one of them.

This paper proposes a new and effective approach to number a compact neighborhood region, i.e., basin of attraction (BOA), of local minima using the unbiased coding rule [11]. Fig. 2 illustrates the relationship between the binary strings and their real values decoded by the unbiased coding rule for an m-bit long binary string inside whose equation is written as:

$$g\left(b_m b_{m-1} \cdots b_1\right) = l + \frac{u-l}{2^{m+1}} \left(\sum_{j=1}^{m} b_j 2^j + 1 \right) \tag{3}$$

where l and u represent the lower and upper bounds in decoding, respectively. As shown in Fig. 2, it is apparent

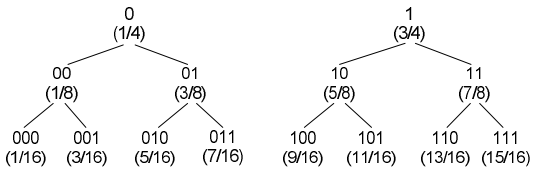

Fig. 2. Binary tree composed of binary strings and their real values decoded by the unbiased coding rule

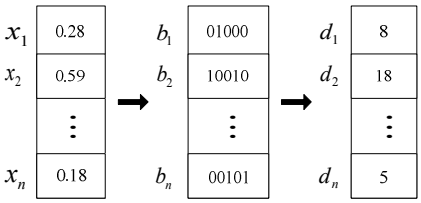

Fig. 3. Region registering process for an n-dimensional real-valued solution vector x

that the decoded values occupy symmetric and non-overlapping positions in the whole domain.

In the present work, a new inverse transformation of the unbiased decoding rule is necessary to map a real-valued search point into its nearest binary string, which represents a corresponding region as well. That is, a search point of 0.6 for instance is nearest to the binary strings 1 (3/4=0.75), 10 (5/8=0.625) or 100 (9/16=0.5625) at each level of string length. Since the string length is proportional to the area resolution, mapping to a smaller region requires a longer string, such as one of length 100.

To this end, (3) is rewritten in order for a real value to be encoded into a binary string with a length of m:

$$y(x)=\left\lfloor \frac{2^{m+1}}{u_x-l_x}(x-l_x)-1 \right\rfloor \approx \sum_{j=1}^{m} b_j 2^j \qquad (4)$$

In an n-dimensional problem, the unbiased coding approximation is carried out for each variable of a point and returns an binary matrix that represents its corresponding region. The binary matrix is then decoded into an integer vector to designate the divided region. Fig. 3 illustrates the example of the region registering process for the n-dimensional point.

2.3 Supervisory multistart with MADS

The supervisory multistart search proposed in this work consists of local searches proceeding from randomly chosen initial points in a parallel manner, collecting information on the local minima and BOA's at each iteration. Since the conventional multistart carries out a local search in a serial manner starting from one of the initial search points until converging to its local minimum and restarting from the other initial point afterwards, the attained local minima can be crowded near the previously found or premature local minima.

This crowding can be avoided in the supervisory multistart by checking the cost value and standard deviation of the trial solutions at each iteration of the search. In MADS, 2n neighborhood points are generated inside the frame of the incumbent point and, thus, the standard deviation of their cost values is a useful indicator of the search status. When the local minimum point is trapped in one of the BOA's, the standard deviation of the neighborhood points will be quite small. To resolve the problem of the different levels of standard deviation in the various cost functions, the standard deviation is normalized by dividing by with the minimum cost of the trial solutions in the present code.

The proposed multistart scheme employs elitism to judge convergence to unacceptable local minima using the information on the previous local minima. That is, once the current search point enters the BOA, its cost function should be smaller than the average of those in the top 30% of the previous local minima. If not, the current search is stopped in the iterative search.

For additional restart from a new search region in the case of failure in the current local search, we examine whether the randomly selected initial point is included in the BOA regions located so far through a look-up table. In this case, MADS restarts from this initial search point. This type of search scheme is called the region decision method (RDM).

The proposed supervisory multistart is written in pseudo-code as follows:

Supervisory multistart with MADS
Initialization:
Generate n_{rst} initial points randomly selected in search domain.
Start MADS from the i th initial point x_0^i. Where, $\boldsymbol{x}_{cb}$ and J_{cb} are the current best point and value, $\boldsymbol{x}_{lm}$ and J_{lm} are the local minimum point and value, $J(\boldsymbol{x})$ is the cost value of function.
$J(x_{lm}^i) = J(x_0^i)$
$k = 0$
while $k <$ max_iter **or** termination condition is not satisfied **do**
$k = k+1$
for $i = 1 : n_{rst}$.
if $\mathbf{x}_{lm}^i$ enters a BOA and $J(\mathbf{x}_{lm}^i) > J_{elite}$ **then**
This point is discarded in this iteration.
else
while $\mathbf{x}_{lm}^i$ is improved **do**
Perform MADS:
Generate trial points $\mathbf{x}_j,\ j = 1,\cdots,2n.$ around $\mathbf{x}_{lm}^i$ with Δ_k^m.
$J_{cb} = \min J(\mathbf{x}_j),\ j = 1,\cdots,2n.$
if $J_{cb} < J_{lm}^i$ **then**
$\boldsymbol{x}_{lm}^i = \boldsymbol{x}_{cb}$.
$J_{lm}^i = J_{cb}$.
$$\Delta_{k+1}^i = \begin{cases} 4\Delta_k^i, & \text{if } \Delta_k^i < \frac{1}{4} \\ \Delta_k^i, & \text{otherwise} \end{cases} .$$
In case of mature convergence, register $\mathbf{x}_{lm}^i$ in search region database.
if termination condition is satisfied **then**
Stop the overall search.
end if
else
$$\Delta_{k+1}^i = \frac{1}{4}\Delta_k^i$$
Stop iteration for $\mathbf{x}_{lm}^i$.
end if
end while
end if
end

end while

3. Benchmark Function

The effectiveness of the proposed algorithms with respect to the local search is validated through two well-known benchmark functions.

The first, Rastrigin function, has the one global minimum and 50 local minima, and is described by the following expression:

$$f_{Ra}(x_1, x_2) = x_1^2 + x_2^2 - \cos(18x_1) - \cos(18x_2) \quad (5)$$

where and the global minimal value is -2, which is located at (0,0).

Fig. 4 shows a comparison of the two global optimization methods applied to the Rastrigin function. Since the global optimization schemes are different from each other, the actual number of local searches is set to 20 in both cases. The 20 individual solutions attained by the conventional MADS called the cost function more times in each local region than the proposed algorithm. Fig. 5 shows the cost profiles of the 20 local minima trajectories with respect to the number of iterations, where it is clear that the proposed method effectively prohibits convergence to unacceptable local minima. In the proposed RDM with MADS, the local search is interrupted in the case of a large difference between the current solution and the best solution found so far. In contrast, the conventional multistart continues MADS until the current mesh size is reduced below the tolerance value, irrespective of the search results attained at the other restart.

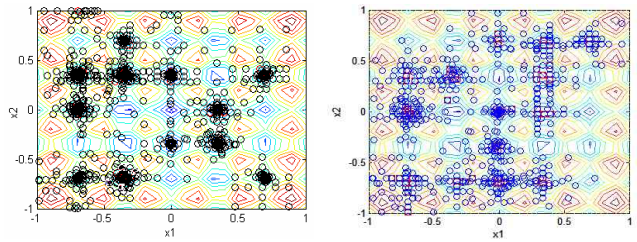

(a) Conventional MADS (b) Proposed algorithms

Fig. 4. Comparison result of Rastrigin function

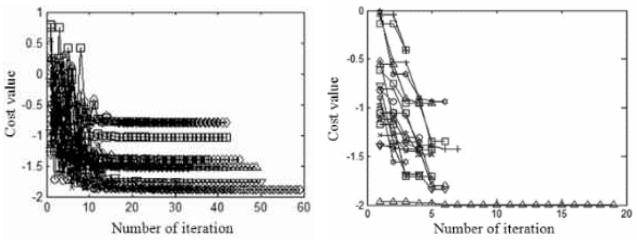

(a) Conventional MADS (b) Proposed algorithms

Fig. 5. Comparison result of iteration number

The second test function, Goldstein-Price function, has one global minimum and several local minima, whose mathematical expression is as follows:

$$\begin{aligned} f_{GP}(x_1, x_2) = & (1 + (x_1 + x_2 + 1)^2 \\ & (19 - 14x_1 + 3x_1^2 - 14x_2 + 6x_1x_2 + 3x_2^2)) \\ & \times (30 + (2x_1 - 3x_2)^2 \\ & (18 - 32x_1 + 12x_1^2 + 48x_2 - 36x_1x_2 + 27x_2^2)) \end{aligned} \quad (6)$$

where, and the global minimal value is 3, which is located at (0,-1).

The five individual solutions attained by the conventional MADS called the cost function more times in each local region than the proposed algorithm. The convergence results of the Goldstein-Price function with the Rastrigin function are shown as function evaluation numbers in Table 1. For the comparison of the numerical performance of the conventional multistart and the proposed method, the local search is carried out 10 times from random initial points with the termination criterion that the difference between the function value of the current global minimum and the acknowledged global minimum value of the benchmark function should be below 10^{-6}. However, the search is terminated if the global minimum has not been found when the mesh size drops below 10^{-8}.

In addition, Table 1 compares the function evaluation numbers counted while the proposed RDM with MADS and other optimization algorithms such as conventional MADS, PSO (Particle Swarm Optimization) [12, 13] and EA (Evolution Algorithm) locate the global minima of the Rastrigin and Goldstein-Price functions, where evaluation number of EA is adapted as in [14]. For the Rastrigin function and Goldstein-Price function, the proposed RDM with MADS reduces the average function evaluation number of the conventional method by 80.2% and 61.8% after 10 restarts, respectively. Consequently, the proposed RDM with MADS is more efficient in global optimization

Table 1. Comparison of function evaluation numbers consumed to locate global minima starting from the same initial points for test functions

Function Name	Restart No.	1	2	3	4	5	6	7	8	9	10	Avg.	Evolution Algorithm
Rastrigin	PSO	1875	1225	750	825	1700	1275	1825	3025	2550	1700	**1675**	**2048**
	Conventional	3300	3268	3128	3196	3068	3320	3132	3284	3172	3096	**3196**	
	Proposed	660	688	672	640	556	676	656	704	620	464	**633**	
Goldstein - Price	PSO	400	530	490	530	790	400	470	430	510	500	**505**	**460**
	Conventional	410	1117	682	530	583	773	1149	749	1297	789	**807**	
	Proposed	353	413	313	309	265	269	253	317	293	305	**309**	

than the conventional multistart with MADS, especially useful for multimodal functions. The proposed algorithm has been employed for optimal design of IPMSG.

4. Optimal Design of IPMSG

4.1 Characteristics of IPMSG

The field flux of IPMSG, which has a rotor structure with PMs buried in it, is generated by PMs without mechanical contact to air gap. This structure enables IPMSG to operate in good system stability and durability. With this advantage, it has a higher power density and efficiency than other types of generators. IPMSG has the outstanding characteristics of the d-q axis inductance difference caused by the magnetic saliency [7], as shown in Fig. 6.

The terminal voltage is controlled analogously to the current combination. Its governing d-q terminal voltage and torque equation can be formulated as follows:

$$V_d = -R_s i_d + L_d \frac{di_d}{dt} - \omega\lambda_q \tag{7}$$

$$V_q = -R_s i_q + L_q \frac{di_q}{dt} + \omega\lambda_d \tag{8}$$

$$T^e = \frac{3}{2}\frac{P}{2}(\lambda_d i_q + \lambda_q i_d) \tag{9}$$

where, R_s is the coil resistance, ω is the mechanical angular speed, λ_d and λ_q are the d-q flux linkages at coil, L_d and L_q are the d-q inductance.

IPMSG usually operates under significant magnetic saturation around the bridge and center posts of the rotor, which should be as small as possible in order to reduce leakage flux; however, small bridge and center posts reduce mechanical strength. Hence, electromagnetic field analysis and mechanical stress analysis based on nonlinear FEA should be carried out in order to evaluate an accurate operating behavior considering the saturation and strength.

4.2 Objective function: Torque-ripple

The IPMSG requires various performance parameters to be taken into consideration, such as the harmonics, efficiency, size, torque ripple, etc. However, it is impossible to optimally design all of these parameters at once [15]. In this paper, minimizing the torque ripple is purposely selected for the objective function. According to Faraday's law, the armature reaction occurs on the stator coils owing to the rotating field formed by the rotor, whereupon the differences of the resultant magnetic field, and cogging torque and reluctance according to the rotor position cause torque ripples. These torque ripples can cause performance degradation, such as low efficiency, harmonics and instability of the system. For these reasons, it can be said that reducing the torque ripple is crucial. The equations for torque ripple and its period are [16]:

$$T^e_{ripple} = \frac{T^e_{Max.} - T^e_{Min.}}{T^e_{Avg.}} \tag{10}$$

$$T^e_{ripple\text{-}period} = \frac{360}{2 \times N_p} \times \frac{2}{P}[mec.Angle] \tag{11}$$

where, $T^e_{Avg.}$ is average torque according to rotor position. $T^e_{Max.}$ and $T^e_{Min.}$ are maximum and minimum torque. N_{ph} and P denote the number of phase and poles.

4.3 Design variables

Due to the many design parameters of the IPMSG, the selection of appropriate design variables is hard work itself. In the optimization process, the computation time increases dramatically as more design variables are selected. Therefore, in order to solve this problem, it is necessary to minimize the number of design variables that critically influence the torque ripple.

Five design parameters are selected for the optimal design, as shown in Fig. 7. The design variables are the dimensions of the PMs (X_1, X_2) angle of the PMs (X_3), depth (X_4) and width (X_5) of the slitting. In the case of a stator with a number of rectangle slots, the size range of design variables is extremely limited by magnetic saturation of the stator, which scarcely affects torque ripple. Hence, the other dimensions including the stator are fixed.

4.4 Constraint variables

In the design of the large-scale IPMSG, a mechanical

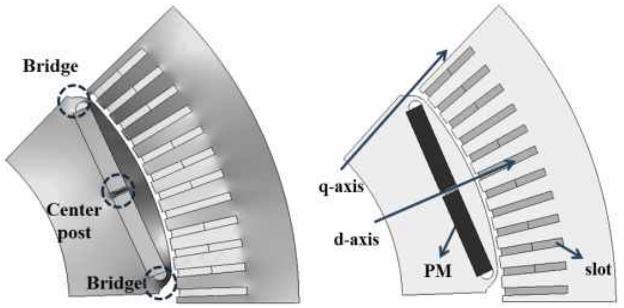

Fig. 6. Magnetic saturation and d-q modeling

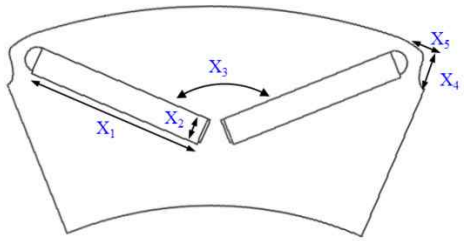

Fig. 7. The design variables of the IPMSG

stress problem arises because of the high centrifugal force caused by the large diameter of the rotor, which causes the breakdown of the generator. In the case of the optimal design, the mechanical stress for each modeling varies greatly according to the change of the geometric dimension of the rotor. In general, maximum mechanical stress by centrifugal force is generated around bridges or center-posts of the rotor, which is designed as a sensitive factor.

The safety factor, which is the tolerance index for the external stress without any strain on the materials, can be formulated as a function of the maximum stress and yield point as follows [9]:

$$safety\ factor = \frac{Yield\ \ Point}{Maximum\ \ stress} \tag{13}$$

It is necessary to maintain the safety factor over a limited range in order to prevent breakdown. The safety factor as constraint variable is selected to maintain over 1.69. At the same time, the torque average over 49 kNm is selected as another constraint variable to satisfy the capacity of IPMSG.

5. Optimal Design Results

5.1 Specification

The IPMSG (5.6MW at 1096rpm) adaptively compatible to a wind turbine is designed optimally with the abovementioned global optimization methods. Table 2 shows the target specifications of the IPMSG.

5.2 Process of optimal design

Fig. 8 shows the flow chart for the optimal design of IPMSG using the proposed RDM with MADS. The electromagnetic modeling and mechanical modeling are designed using the design variables obtained from the optimization algorithm. In the case of the electromagnetic analysis, both the rotor and stator modelling are required. However, in the case of the mechanical stress analysis, only the rotor modeling is required, because the centrifugal force affects only the rotor. After the analysis of these terms, performance evaluation of the average torque and safety factor is conducted. The torque ripple is calculated and reserved when the average torque and safety factor satisfy both conditions. If those are not satisfied, it can be judged that the torque ripple adopted seems higher than that in other designs. Therefore, the best candidate for designing the required level of torque ripple can be achieved after all.

Table 2. The specifications of the IPMSG

Poles / slots		8 / 96
Stator outer / inner diameter		1200 mm / 860 mm
Rotor outer / inner diameter		850 mm / 500 mm
Stack length		965 mm
Rated power / voltage		5.6 MW / 3300 V_{rms}
Rated speed / frequency		1096 rpm / 73 Hz
Constraint	Avg. torque	Over 49 kNm
	Safety factor	Over 1.69
Core	Material	50PN470
	Yield point	265 Mpa

5.3 Analysis and results

The torque ripple results are plotted against the number of iterations for the proposed algorithm with 20 multistart points in Fig. 9.

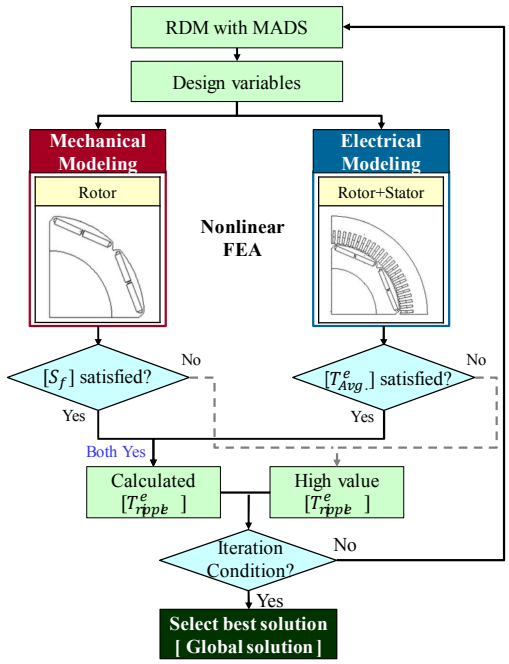

Fig. 8. Flow chart of the proposed algorithm applied to the optimal design of the IPMSG

Table 3. Comparison results of optimal design. (S/W:JMAG, number of elements : 31,000~33,000)

Classification		X1 [mm]	X2 [mm]	X3 [deg]	X4 [mm]	X5 [mm]	Call No.	Computational Time [hr]	Torque avg. [kNm]	Safety factor	Torque ripple [%]
Conventional model		131	20	135	28.63	30	-	-	49.5	1.69	6.67
RDM with MADS	Best	132.92	19.44	138.92	2.74	21.98	1475	40.15	49.1	2.88	2.18
	Second	132.95	21.11	139.32	2.77	18.12			49.6	2.52	2.21
	Third	132.98	26.92	139.52	2.80	21.68			51.2	2.04	2.31
Conventional MADS		132.89	19.57	139.01	2.75	20.47	4217	114.80	49.1	2.87	2.19
PSO		133.12	20.38	139.42	2.76	20.35	2000	54.44	49.5	2.48	2.20

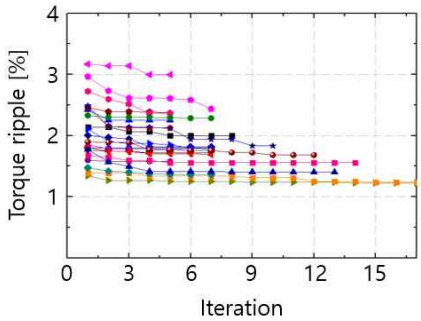

Fig. 9. The torque ripple vs. the number of iterations

The multistarted individual solutions terminate rapidly under the following three conditions: 1. Trapping of BOA, 2. A relatively higher cost value concerning torque ripple than other solutions, 3. No improvement in the solution observed during further iterations. This means that the probability of a global optimum is low for the present solution, which has a significant effect on the excessive computation time.

Table 3 shows a comparison of the conventional model and the optimal models in terms of torque ripple and evaluation numbers, where the top three optimal models are presented by the proposed algorithm. Especially, the proposed algorithm is compared with conventional MADS and PSO, and the call number of PSO is set 2000 times. Although conventional MADS and PSO cost more call numbers, their torque ripple is not better than the best solution of the proposed algorithm. Among the design variables, the depth (x_4) of the slitting is the main factor with the most significant changes compared to the conventional model. These dimensions are similar between optimal models.

In terms of torque ripple, the best model (2.18%) is more improved than the conventional model (6.67%). The torque ripple waveform of the optimally designed one is compared with that of the conventional model, as shown in Fig. 10. It can be seen that the torque pulsation of the optimally designed one disappears noticeably according to the rotational mechanical angle, which will promise not only to reduce the noise and vibration, but also increase the stability.

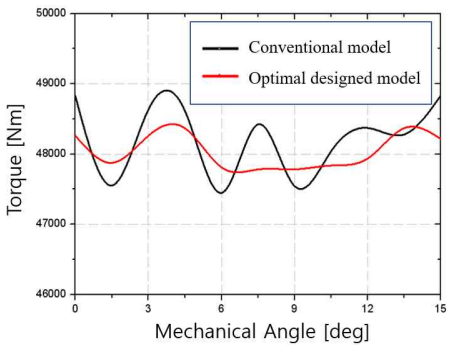

Fig. 10. The torque ripple waveform

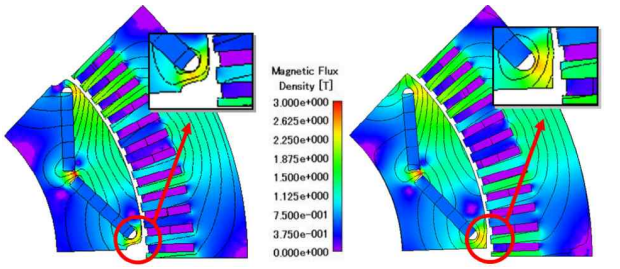

(a) Conventional model (b) Optimally designed model

Fig. 11. Magnetic flux density distribution.

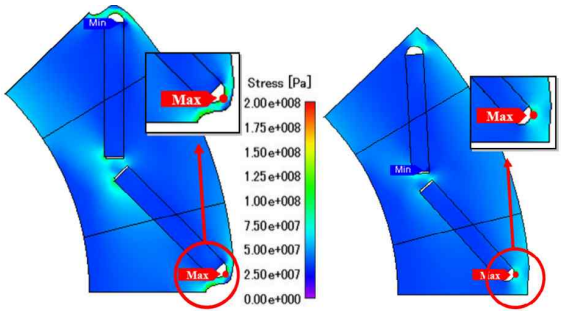

(a) Conventional model (b) Optimally designed model

Fig. 12. Mechanical stress distribution

Fig. 11 and Fig. 12 show comparison results of the flux density distribution and mechanical stress analysis between the conventional model and optimally designed model. As shown in Figures, the bridge of the optimally designed model is bigger than that of the conventional model, leading to a slight decrease of the average torque due to the leakage flux on the bridge. However, both torque ripple (2.18%) and mechanical stress (2.88) intensity have been improved in the optimally designed model.

6. Conclusion

In this paper, RDM with MADS was newly introduced and employed for the optimal design of a 5.6MW IPMSG minimizing the torque ripple. The RDM with MADS proposed local searches proceeding at each multistart in a parallel manner. It can effectively reduce the function calls by avoiding revisits and checking the cost standard deviation at each iteration of the search. Its reliability and fast convergence were clarified with evaluation of the benchmark functions and the optimal design of an IPMSG. In particular, the optimal design of the IPMSG has been coupled with the mechanical stress analysis to prevent breakdown caused by centrifugal force. The optimal design result of the proposed algorithm shows its superiority in terms of the torque ripple, mechanical stress, and the effectiveness of the optimization algorithms. Above all, the feasibility of the proposed optimal design methodology considering the mechanical stress will provide more reliable analysis and results in designing the electrical machines.

References

[1] Baoquan Kou, Yinru Bai and Liyi Li, "A Novel Wind Power Generator System with Automatic Maximum Power Tracking Capability," *IEEE Trans. Energy convers.*, vol. 28, no. 3, pp. 969-978, Sept. 2013.

[2] Zac Mouton and Maarten J. Kamper, "Modeling and Optimal Design of an Eddy Current Coupling for Slip-Synchronous Permanent Magnet Wind Generators," *IEEE Trans Ind. Electron.*, vol. 61, no. 7, pp. 3367-3376, July 2014.

[3] C.Audet, J. E. Dennis Jr, "Mesh adaptive direct search algorithms for constrained optimization," *SIAM J. Optim.*, vol. 17, no. 1, pp. 188-217, 2006.

[4] Dongsu Lee, Seungho Lee, Jong-Wook Kim, Cheol-Gyun Lee and Sang-Yong Jung, "Intelligent memetic algorithm using GA and guided MADS for the optimal design of Interior PM synchronous machin," *IEEE Trans. Magn.*, vol. 47, no. 5, pp. 1230-1233, May 2011.

[5] Dongsu Lee, Jong-Wook Kim, Cheol-Gyun Lee and Sang-Yong Jung, "Variable mesh adaptive direct search algorithm applied for optimal design of electric machines based on FEA," *IEEE Trans. Magn.*, vol. 47, no. 10, pp. 3232-3235, Oct. 2011.

[6] Seungho Lee, Yu-Seok Jeong, Yong-Jae Kim and Sang-Yong Jung, "Novel analysis and design methodology of interior permanent magnet synchronous motor using newly adopted synthetic flux linkage," *IEEE Trans Ind. Electron.*, vol. 58, no. 9, pp. 3806-3814, Sept. 2011.

[7] Geun-Ho Lee, Sung-Il Kim, Jung-Pyo Hong and Ji-Hyung Bahn, "Torque Ripple Reduction of Interior Permanent Magnet Synchronous Motor Using Harmonic Injected Current," *IEEE Trans. Magn.*, vol. 44, no. 6, pp. 1582-1585, June 2008.

[8] Hong Guo, Zhiyong Wu, Hao Qian, Kaiping Yu and Jinquan Xu, "Statistical analysis on the additional torque ripple caused by magnet tolerances in surface-mounted permanent magnet synchronous motors," *IET Electr. Power Appl.*, vol. 9, no. 3, pp. 183-192, Mar. 2015.

[9] Jae-Woo Jung, Byeong-Hwa Lee, Do-Jin Kim, Jung-Pyo Hong, Jae-Young Kim, Seong-Min Jeon and Do-Hoon Song, "Mechanical Stress Reduction of Rotor Core of Interior Permanent Magnet Synchronous Motor," *IEEE Trans. Magn.*, vol. 48, no. 2, pp. 911-914, Feb. 2012.

[10] Youngjun Ahn, Jiseong Park, Cheol-Gyun Lee, Jong-Wook Kim and Sang-Yong Jung, "Novel Memetic Algorithm implemented With GA (Genetic Algorithm) and MADS (Mesh Adaptive Direct Search) for Optimal Design of Electromagnetic System," *IEEE Trans. Magn.*, vol. 46, no. 6, pp. 1982-1985, Feb. 2010.

[11] Jong-Wook Kim, Taegyu Kim, Youngsu Park and Sang Woo Kim, "On load motor parameter identification using univariate dynamic encoding algorithm for searches (uDEAS)," *IEEE Trans. Energy convers.*, vol. 23, no. 3, pp. 804-813, sept. 2008.

[12] Abdallah Chanane, Ouahid Bouchhida and Hamza Houassine, "Investigation of the transformer winding high-frequency parameters identification using particle swarm optimisation method," *IET Electr. Power Appl.*, vol. 10, no. 9, pp. 923-931, Nov. 2016.

[13] Hong Guo, Zhiyong Wu, Hao Qian and Zedong Sun, "Robust design for the 9-slot 8-pole surface-mounted permanent magnet synchronous motor by analytical method-based multi-objectives particle swarm optimization," *IET Electr. Power Appl.*, vol. 10, no. 2, pp. 117-124, Feb. 2016.

[14] Yong, L., Lishan, K. and Evans, D.J., "The annealing evolution algorithm as function optimizer," *Parallel Computing*, vol. 21, no. 3, pp. 389-400, 1995.

[15] Jianing Yin, Xiaoyong Zhu, Li Quan, Chao Zhang and Zixuan Xiang, "Comprehensive multi-objective scalarisation optimisation of a permanent magnet machine with correlation parameters stratified method," *IET Electr. Power Appl.*, vol. 11, no. 1, pp. 72-79, Jan. 2017.

[16] C. Sahin, A. E. Amac, M. Karacor and Ali Emadi, "Reducing torque ripple of switched reluctance machines by relocation of rotor moulding clinches," *IET Electr. Power Appl.*, vol. 6, no. 9, pp. 753-760, Nov. 2012.

Dongsu Lee He received the B.S degree in electrical engineering from Donga University, Busan, Korea in 2010 and the M.S. and Ph.D. degrees in electrical and computer engineering from Sungkyunkwan University, Suwon, Korea in 2013 and 2016, respectively. He is currently a Researcher with the Department of Electrical and Computer engineering, University of Illinois at Urbana-Champaign, Urbana, USA. His research interests include the numerical analysis and optimal design of electric machines and power apparatus.

Byungkwan Son He received the B.S. degree in electronic and electrical engineering in 2014 from Sungkyunkwan University, Suwon, South Korea, where he is currently working toward the Ph.D. degree in the Department of Electronic, Electrical and Computer Engineering. His research interests include numerical analysis and design optimization of electric machine and power apparatus.

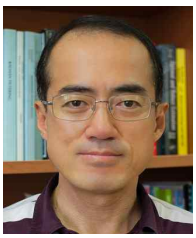

Jong-Wook Kim He received the B.S., M.S., and Ph.D. degrees from the Electrical and Computer Engineering Division at Pohang University of Science and Technology (POSTECH), Pohang, Korea, in 1998, 2000, and 2004, respectively. He is currently a Associate Professor in the Department of Electronics Engineering at Dong-A University, Busan, Korea. His current research interests are numerical optimization methods, embedded system, intelligent robot control.

Sang-Yong Jung He received the B.S., M.S., and Ph.D. degrees in electrical engineering from Seoul National University, Seoul, Korea, in 1997, 1999, and 2003, respectively. From 2003 to 2006, he was a Senior Research Engineering with the R&D Division, Hyundai Motor Company, Korea, and the R&D Division, Kia Motor, Korea. From 2006 to 2011, he was an Assistant Professor with the Department of Electrical Engineering, Dong-A University, Busan, Korea. Since 2011, he has been an Associate professor with the Department of Electrical and Computer Engineering, Sungkyunkwan University, Suwon, Korea. His research interests include the numerical analysis and optimal design of electric machines and power apparatus.